Stability and string stability of car-following models with reaction-time delay

Guy Fayolle, Jean-Marc Lasgouttes, Carlos Flores

STABILITY AND STRING STABILITY OF CAR-FOLLOWING MODELS WITH REACTION-TIME DELAY

GUY FAYOLLE*, JEAN-MARC LASGOUTTES*, AND CARLOS FLORES†

Abstract. We investigate the transfer function emanating from the linearization of a car-following model for human drivers, when taking into account their reaction time, which is known to be a cause of the stop-and-go traffic phenomenon. This leads to a non rational transfer function, implying nontrivial stability conditions which are explicitly given. They are in particular satisfied whenever string stability holds. We also show how this reaction time can introduce a *partial string stability*, where the transfer function modulus remains smaller than 1 up to some critical frequency. We explore conditions in the parameter space discriminating between 3 different regimes (stability, string stability, partial string stability).

Key words. Car-following model, traffic control, transportation networks, stability of linear systems, methods of the complex variable.

1. Introduction. It has been known for some time, and even demonstrated in the field [22, 23], that vehicles on a highway can suffer from stop-and-go traffic conditions without any external intervention. To explain this phenomenon, traffic evolution is studied at a microscopic level and further expanded as a series of interconnected systems named car-following models. These refer to the way drivers maintain a spacing gap towards the preceding vehicle. In other words, car-following models predict the motion of a human-driven vehicle in a vehicular stream, by studying the dynamics of the inter-vehicle gap.

Conceptualized for the first time by Pipes [18] and Chandler *et al.* [4], several car-following models have been proposed in the literature to simulate mathematically the driving behavior at a microscopic level. The review of car-following models in [26] highlights five groups: Gazis-Herman-Rothery [8] (GHR, also known as GM model), collision-avoidance models, linear models, psycho-physical or action-point models and fuzzy logic-based models.

Over the years, the aforementioned models served as a basis for more complex and accurate models. Gipps' car-following model [10], has been widely used, both in research and practice, for its accuracy. The Optimal Velocity Model of Bando *et al.* [2] described the dynamics as an attempt to attain a prescribed speed that depends on distance to the leader vehicle. Later, Treiber *et al.* [29] introduced the Intelligent Driver Model (IDM), which gained a lot of attention, becoming the most popular car-following model for human drivers. In [28], IDM was extended to take into account driver's adaptation effect using memory functions. More recently, IDM+ has been proposed for traffic flow study [21].

Several authors claimed that reaction-time delays of the human driver should be considered to represent more accurately upstream wave propagation in a traffic lane. For instance, stop-and-go traffic jams have been shown to be connected to these delays in [12–14], demonstrating that an unexpected deceleration of the front vehicle is followed by an even stronger ego-deceleration to avoid rear-end collision. This amplification of vehicle states along a string can lead to a traffic jam. An analysis of such a delayed car-following model on a circle can be found in [15].

Studies on traffic stability (e.g. [6, 31]) are often set in traffic conditions naturally

*RITS project-Team, Inria, *firstname.lastname*@inria.fr.

†California PATH program of the Institute of Transportation Studies, UCB, carfloresp@berkeley.edu

exhibiting string instability, which in terms of transfer function means that any excitation of a frequency below a certain limit is amplified. We are interested here in a slightly different setting, where reaction time is taken into account for human drivers. In this context, we provide explicit conditions under which the underlying differential system is unstable. Moreover, an interesting regime appears, where string instability only concerns frequencies in a particular band.

The paper is organized as follows: after describing the model in Section 2, the stability domain of the linearized version is given in Section 3 as well as its relation to string stability in Section 4. We introduce the notion of *partial string stability* in Section 5 and provide various conditions under which it can take place. Section 6 is devoted to numerical computation in the case of IDM, enlighting a range of parameters where partial string stability occurs. Finally, Section 7 discusses control strategies made possible by partial string stability and shows how these results form the basis of a broader traffic stabilization vision.

2. The model. We start from a classical *car-following model* on a line with identical vehicles, in which we introduce a reaction time τ for each driver. For simplicity of presentation, we follow the notation and the development of [31]. Let $x_j(t)$ be the position of vehicle j along the road at time t, $v_j(t)$ its speed and $a_j(t)$ its acceleration. We assume that vehicle j obeys a car-following model of the form

$$\begin{aligned} a_j(t+\tau) &= f(x_{j-1}(t) - x_j(t), v_{j-1}(t) - v_j(t), v_j(t)) \\ &\stackrel{\text{def}}{=} f(\Delta x_j(t), \Delta v_j(t), v_j(t)), \end{aligned} \tag{2.1}$$

where f is a continuously differentiable function on $\mathbb{R}^3$. The acceleration at time t thus depends on the following variables, delayed by τ: the distance to the vehicle in front, their relative speed and the speed of vehicle j itself. In the case where there is no reaction time ($\tau = 0$), most models described in the previous section (GHR model, Gipps' model, OVM, IDM, IDM+) are special cases of (2.1).

Note that the GHR model does rely on a reaction-time delay, but, in this case, the last parameter of f is $v_i(t+\tau)$ instead of $v_i(t)$: it is considered that the driver knows his own speed in real time.

The relation at equilibrium between the heading Δx^* and the speed v^* is given by the equation

$$0 = f(\Delta x^*, 0, v^*). \tag{2.2}$$

Solving the equation yields the optimal inter-vehicle distance Δx^* for a given speed v^*. Equation (2.1) is formally intractable in general; a fruitful method consists in a linearization around the equilibrium point $(\Delta x^*, 0, v^*)$:

$$a_j(t+\tau) = k_{dx}(\Delta x_j(t) - \Delta x^*) + k_{dv}\Delta v_j(t) + k_v(v_j(t) - v^*). \tag{2.3}$$

The parameters k_{dv}, k_{dx}, k_v are positive and stand for the following partial derivatives at equilibrium

$$k_{dx} = \frac{\partial f}{\partial \Delta x}, \qquad k_{dv} = \frac{\partial f}{\partial \Delta v}, \qquad k_v = -\frac{\partial f}{\partial v}.$$

An explicit computation of these constants is carried out for IDM in Section 6.

Equation (2.3) defines a second-order linear differential equation for the positions of the vehicles. For all $\Re(s) \geq 0$, let $V_j(s)$ denote the Laplace transform of $v_j(t) - v^*$.

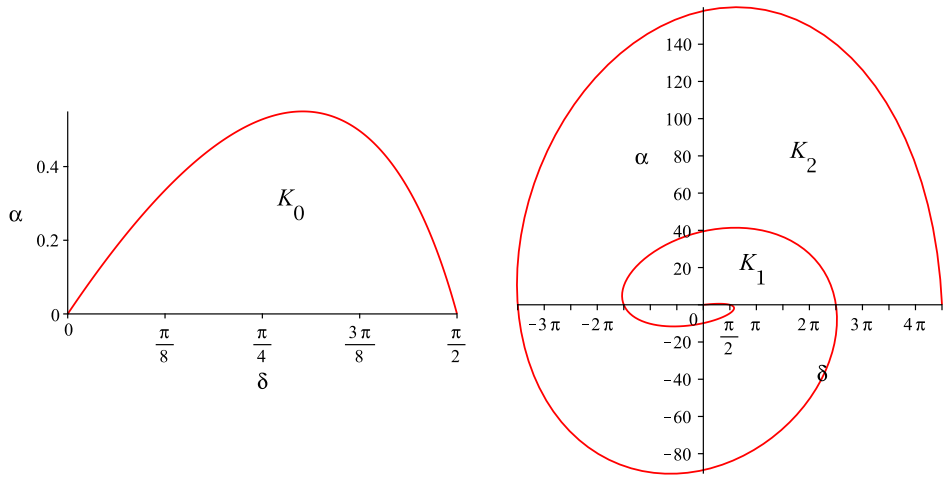

FIG. 3.1. *Left: stability region K_0 in terms of the parameters α and δ. Right: the spiral (3.1) represented for $y \in [0, \frac{9\pi}{2}]$; note that the stability region K_0 of the left panel is barely visible in the display of the right panel.*

Then the fundamental transfer function takes the form

$$T(s) \stackrel{\text{def}}{=} \frac{V_j(s)}{V_{j-1}(s)} = \frac{k_{dv}s + k_{dx}}{s^2 e^{s\tau} + (k_{dv} + k_v)s + k_{dx}}, \quad \Re(s) \geqslant 0, \tag{2.4}$$

For mathematical convenience, we introduce the scaling,

$$z = s\tau, \quad \alpha = \tau^2 k_{dx}, \quad \beta = \tau k_{dv}, \quad \gamma = \tau k_v, \quad \delta = \beta + \gamma. \tag{2.5}$$

Then (2.4) can be rewritten as

$$Q(z) = T\Big(\frac{z}{\tau}\Big) = \frac{\beta z + \alpha}{D(z)}, \quad \text{where } D(z) = z^2 e^z + \delta z + \alpha. \tag{2.6}$$

Note that, unlike in [31], $Q(z)$ is no more a rational but a transcendental function, because of the term e^z. As we shall see in the next sections, the analysis and the behavior of the system become more intricate.

3. Stability region. The first basic question about the dynamics of (2.3) concerns its stability.

DEFINITION 3.1 (Stability). *The system is* stable *if and only if $Q(z)$ has no pole in the region $\Re(z) \geq 0$.*

The physical meaning of this property is that a finite perturbation of x_i should never have an unbounded effect. Note that stability always holds when $\tau = 0$ as in [6, 31].

The goal of this section is to state necessary and sufficient conditions for the system to be stable. They are nontrivial due the presence of the reaction time τ. Interestingly, we shall see that they only depend on α and $\delta = \beta + \gamma$, but not on the individual values of β and γ.

We want to analyze the poles of $Q(z)$ in the region $\Re(z) \geqslant 0$. The function $D(z)$ belongs to the class of so-called exponential polynomials, and many works have

been devoted to studying the zeros of these polynomials. The following intermediate proposition describes the possible zeros of $D(z)$ (defined by (2.6)) on the imaginary axis.

PROPOSITION 3.2. *In the (δ, α) plane, let $\mathcal{L}$ be the curve shown in Fig. 3.1, given in the parametric form*

$$\begin{cases} \delta = y \sin y, \\ \alpha = y^2 \cos y, \end{cases} \quad y \geq 0, \tag{3.1}$$

and let $\mathcal{L}_j$, $j \geq 0$, be the arcs of $\mathcal{L}$ corresponding to $y \in [0, \pi/2] + 2j\pi$.

Then any real solution in y of (3.1) corresponds to a zero of $D(iy)$. Moreover, in the parameter space, the system (3.1) is equivalent to the algebraic differential equation

$$\frac{d\alpha}{d\delta} = \frac{4\alpha - \delta(\delta^2 + \sqrt{\delta^4 + 4\alpha^2})}{2(\alpha + \delta)}, \tag{3.2}$$

subject to the initial conditions $\alpha(0) = 0$ with $\alpha'(0) = 1$.

It is worth remarking that the curve $\mathcal{L}$, parametrized by (3.1), looks like an Archimedean spiral, the spires of which are dilated along the α-axis in the (δ, α)-plane.

Proof. Consider the imaginary axis $\{z = iy, y \in \mathbb{R}\}$, where D defined by (2.6) may have two conjugate zeros at the points iy_0 and $-iy_0$. Then

$$D(iy_0) = -y_0^2 \cos y_0 + \alpha + iy_0(-y_0 \sin y_0 + \delta) = 0$$

yields

$$\begin{cases} y_0^2 \cos y_0 = \alpha, \\ y_0 \sin y_0 = \delta, \end{cases}$$

which coincides exactly with system (3.1). In addition, when y_0 exists, it is immediate to check that, necessarily,

$$y_0 = \left(\frac{\delta^2 + \sqrt{\delta^4 + 4\alpha^2}}{2} \right)^{\frac{1}{2}} > \delta. \tag{3.3}$$

Viewing now in (3.1) the quantities y_0 and α as functions of δ, one gets by differentiation

$$\begin{cases} \dfrac{dy_0}{d\delta}(2y_0 \cos y_0 - y_0^2 \sin y_0) = \dfrac{d\alpha}{d\delta}, \\ \dfrac{dy_0}{d\delta}(\sin y_0 + y_0 \cos y_0) = 1, \end{cases}$$

so that

$$\frac{d\alpha}{d\delta} = \frac{2\alpha - \delta y_0^2}{\alpha + \delta},$$

which is exactly equivalent to (3.2) by using (3.3). It is important to observe that the differential equation (3.2) has the classical form

$$\frac{d\alpha}{d\delta} = F(\delta, \alpha), \quad \forall (\delta, \alpha) \in \Delta \in \mathbb{R}^{+2},$$

where Δ is a finite domain including the point $(0,0)$, where $F(\delta,\alpha)$ is *not continuous, and nor does satisfy a classical Lipschitz condition with respect to* α.

On the other hand, whenever system (3.1) holds, we obtain the immediate following relationships.

1. $\alpha'(0) = \lim_{\delta\to 0} \frac{\alpha}{\delta} = 1$.
2. If $\alpha = 0$, then either $\delta = 0$ or $\delta = \frac{\pi}{2} + 2k\pi$, for any integer $k \geq 0$.
3. If $\delta = 0$, then $\alpha = (2\ell\pi)^2$, for any integer $\ell \geq 0$.

The proof of the proposition is terminated. ∎

Although a part of the next theorem is quoted in [3, section 13.9] with a reference to [20], we propose an original self-contained proof of the stability conditions, including a precise enumeration of the zeros of $D(z)$ in the region $\Re(z) \geq 0$. *The method relies on complex analysis and on a powerful argument of continuity with respect to the parameters* (δ,α), and is applicable to more general transfer functions.

THEOREM 3.3. *The system is stable if and only if the couple of parameters* (α,δ) *belongs to the finite open domain* K_0*, bounded by the curve* $\mathcal{L}_0$ *and the open segment* $]0,\pi/2[$ *on the* δ*-axis.*

Moreover, in the positive quarter plane (δ,α)*, let* K_j*,* $j \geq 1$*, be the positive sector lying between* $\mathcal{L}_{j-1}$ *(included) and* $\mathcal{L}_j$ *(not included), see Fig. 3.1. Then, when* $(\delta,\alpha) \in K_j$*, the function* $D(z)$ *has exactly* $2j$ *conjugate zeros with positive real parts.*

We shall use the so-called Rouché's theorem, which we recall below for the sake of completeness.

THEOREM 3.4 (Rouché, see e.g. [25]). *For any two complex-valued functions* f *and* g *holomorphic inside some region* $\mathcal{H}$ *with simple closed contour* $\partial\mathcal{H}$*, if* $|g(z)| < |f(z)|$ *on* $\partial\mathcal{H}$*, then* f *and* $f+g$ *have the same number of zeros inside* $\mathcal{H}$*, where each zero is counted with its multiplicity.*

To find the conditions ensuring the existence and position of zeros for the function D in the right half-plane $\Re(z) \geq 0$, we need two preparatory lemmas.

LEMMA 3.5. *In the right half-plane, let the closed contour* $C(\delta,R)$ *consisting of the two semicircles centered at the origin of respective radii* R *and* δ*, plus the two segments of the imaginary axis* $[i\delta, iR]$ *and* $[-iR, -i\delta]$ *respectively. Henceforth,* R *will stand for a large positive number. Then, for all* (α,δ) *in the region* $0 < \alpha < \delta^2 < 1/4$*, the following inequality holds.*

$$|z^2 e^z + \delta z| > \alpha, \quad \forall z \in C(\delta,R). \tag{3.4}$$

Proof. Inequality (3.4) is evidently satisfied for z on the semicircle of radius R. The situation for the remaining components of the contour is twofold.

(i) $z \in [i\delta, iR] \cup [-iR, i\delta]$. Setting $z = iy$, y real,

$$|ze^z + \delta|^2 = y^2 - 2\delta y \sin y + \delta^2 \geq (1-2\delta)y^2 + \delta^2 > \delta^2$$

(ii) z belongs to the semicircle of radius δ, that is $z = \delta e^{i\theta}, -\pi/2 \leq \theta \leq \pi/2$. Setting $Y \stackrel{\text{def}}{=} e^{\delta\cos\theta} \geq 1$, we get directly

$$|ze^z + \delta|^2 = \delta^2\big[Y^2 + 2Y\cos(\theta + \delta\sin\theta) + 1\big]. \tag{3.5}$$

By the monotony of the sine and cosine functions, we have

$$\cos(\theta + \delta\sin\theta) > \cos(\pi/2 + \delta) = -\sin\delta, \ \ \forall\theta \in [0,\pi/2],$$

and (3.5) yields

$$|ze^z + \delta|^2 > 2\delta^2(1 - \sin\delta).$$

Finally, for $0 < \alpha < \delta^2 < 1/4$, (3.4) holds everywhere on $C(\delta, R)$, and the lemma is proved. ∎

The next lemma is a sharp application of Rouché's theorem.

LEMMA 3.6. *For all $\alpha > \delta^2(e^{2\delta} - 1)^{1/2}$, the equation*

$$z^2e^z + \delta z + \alpha = 0$$

has no roots in the half-disk $z = \rho e^{i\theta}$, $0 \le \rho \le \delta$ and $\theta \in [-\pi/2, \pi/2]$ in the right half-plane.

Proof. By Rouché's theorem, it suffices to establish on the contour of this half-disk the inequality

$$|\delta z + \alpha| > |z^2e^z|. \tag{3.6}$$

Letting $z = x + iy$, we analyze separately the two components of the domain.

(i) On the diameter of the half-disk, $x = 0$ and

$$|\delta z + \alpha|^2 - |z^2e^z|^2 = \delta^2y^2 + \alpha^2 - y^4 > 0, \quad 0 \le |y| \le \delta,$$

which shows (3.6).

(ii) $z = \delta e^{i\theta}, \theta \in [-\pi/2, \pi/2]$. Here,

$$|\delta z + \alpha|^2 = \delta^4 + 2\alpha\delta x + \alpha^2, \quad \text{and} \quad |z^2e^z|^2 = \delta^4e^{2x}.$$

Now, as $0 \le x \le \delta$, (3.6) will plainly be satisfied by choosing for instance

$$\alpha^2 > \delta^4(e^{2\delta} - 1),$$

and the proof of the lemma is terminated. ∎

Proof of Theorem 3.3. There are two main issues: first the stability itself, which concerns only the parameter region K_0; second, the localization of the zeros of $D(z)$ corresponding to the parameter regions $K_j, j \ge 1$.

Proof of stability. Putting together the results of Lemmas 3.5 and 3.6, we conclude at once that $D(z)$ has no zeros in the right half-plane for the parameter region

$$\left\{\delta^2(e^{2\delta} - 1)^{1/2} < \alpha < \delta^2 < \frac{1}{4}\right\},$$

which clearly lies in the interior of K_0. On the other hand, by the principle of the argument (see e.g, [16]), the number of zeros of $D(z)$ can be expressed by means of a Cauchy type integral

$$\frac{1}{2i\pi}\int_{\mathcal{U}} \frac{D'(t)}{D(t)}dt,$$

$\mathcal{U}$ being the boundary of the semicircle of radius R in the right half-plane. *This integral takes integer values and is continuous with respect to (δ, α), as long as $D(z)$ does not vanish on the contour.* For large R, this can occur only on the imaginary axis, implying

$$D(iy) = (\alpha - y^2\cos y) + iy(\delta - y\sin y) = 0, \quad y \in \mathbb{R},$$

which is equivalent to (3.1). Hence, $D(z)$ has no zeros in the region $\Re(z) \ge 0$ if (δ, α) belongs to the interior of the parameter domain K_0, which is a sufficient condition of stability. In the next paragraph, we show that this condition is also necessary.

The zeros of $\mathcal{D}(z)$ in the region $\Re(z) \geq 0$, for the parameter domain $K_j, j \geq 1$. In the parameter space, take a point $P = (\delta, \alpha) \geq (0,0)$ located inside K_j and let P move to the boundary of K_j, to enter K_{j+1}, so that system (3.1) holds, which means that two zeros of $D(z)$ appear on the imaginary axis in the z-plane. These conjugate zeros come from the left half-plane and all what we have to show is that their real part becomes strictly positive when P switches from K_j to K_{j+1}. We deal with the case $j = 0$, the argument being the same for all j.

Let P reach the boundary of K_0 to enter K_1 via the point $(\pi/2, 0)$, and suppose for a while that α is an arbitrary positive function of δ, locally differentiable around $\delta = \pi/2$, with a derivative $q \stackrel{\text{def}}{=} \alpha'(\pi/2) > -\pi^2/4$ (the value of the slope of the curve $\mathcal{L}_0$ at $\delta = \pi/2$) to ensure that the point $P = (\pi/2 + \varepsilon, \varepsilon q)$ belongs to K_1 for ε sufficiently small. Then the possible zeros of $D(z)$ are locally differentiable with respect to δ around $\delta = \pi/2$, whence, by taking the derivative of $D(z) = 0$ and writing $z'(\delta) = \frac{dz}{d\delta}$,

$$z'(\delta)[ze^z(z+2) + \delta] + z + \alpha'(\delta) = 0. \tag{3.7}$$

Instantiating $\delta = \pi/2$ in (3.7), we have $z = \pm i\pi/2$. Choosing for example $z = i\pi/2$, we obtain

$$z'(\pi/2) = \frac{q + i\pi/2}{\pi(1 + i\pi/4)} = \frac{q + \pi^2/8 + i\pi(1 - q/2)/2}{\pi(1 + \pi^2/16)},$$

and the real part of $z'(\pi/2)$ is positive as soon as $q + \pi^2/8 > 0$. Thus, when the point P enters K_1, two conjugate zeros of $D(z)$ come into the right complex half-plane. A similar phenomenon occurs when P passes from K_j to K_{j+1}, creating two additional zeros of $D(z)$ in the right. The proof of the theorem is terminated. ∎

Remark 3.7. We always assumed $\alpha > 0$. For the sake of completeness, let us briefly analyze the case $\alpha = 0$, although it is of little physical interest, since it implies $k_{dx} = 0$. Here, by (2.6), we are left with the analysis of the simpler equation

$$ze^z + \delta = 0,$$

the general solution of which is $W(-\delta)$, the special Lambert W-function, see e.g. [5]. $W(z)$ has an infinite number of branches classically denoted by $W(k, z), k$ integer, and exactly one of them, $W(0, w)$, is analytic around the origin and given by

$$W(0, w) = \sum_{n=1}^{\infty} \frac{(-n)^{n-1} w^n}{n!},$$

where the series is convergent for $|w| \leq e^{-1}$. In particular, $W(0, -\delta)$ does not vanish in the interior of the disk of radius e^{-1}. The curves separating the branches are

$$\{-y \cot y + iy : 2k\pi < \pm y \leq (2k+1)\pi\}, \quad \text{for } k \geq 1.$$

These curves form the images of the negative real axis under the branches $W(k, z)$. As in the case $\alpha > 0$, we have

$$\Re[W(k, -\delta)] < 0, \quad 0 < \delta < \pi/2, \ \forall k = 0, \pm 1, \ldots,$$

and $Q(z)$ has no poles for $\delta \in [0, \pi/2]$.

4. String stability. Stability, as described in Section 3, concerns a single vehicle. As far as groups of vehicles are at stake, even if the system is stable, another issue may appear. Consider for example a string of n identical vehicles where, for some $y \in \mathbb{R}$, $|Q(iy)| > 1$. In this case, since

$$V_j(iy) = Q^n(iy)V_{j-n}(iy), \quad \forall 1 \leq j \leq n,$$

small perturbations could be amplified as they propagate in upstream direction. A metric has been introduced in the literature that relates on how systems' states energy is propagated element-wise in a string of systems. It is referred to as *string stability* [19, 24].

DEFINITION 4.1 (String stability). *The system is called* string stable *if and only if* $|Q(iy)| \leq 1$ *for all* $y \in \mathbb{R}$.

THEOREM 4.2. *String stability implies stability, that is* $(\delta, \alpha) \in K_0$.

Proof. Assume for some parameter region (α, δ, β) string stability holds. This is equivalent to say that, for $z = iy$ on the imaginary axis,

$$|D(iy)| > |\alpha + i\beta y|, \quad y \geq 0.$$

Choose $R > 0$ sufficiently large such that

$$|D(z)| > |\beta z + \alpha|, \quad \forall |z| \geq R.$$

Then $D(z)$ and $D(z) - (\beta z + \alpha) \stackrel{\text{def}}{=} E(z) = z(ze^z + \gamma)$ have, by Rouché's theorem, the same number of zeros in the closed region $\mathcal{V}$ bounded by the curve $\mathcal{U}$ introduced in the stability proof of Theorem 3.3. Note that, for all $z = x + iy, x \geq 0$, we have

$$\Re[D(z)] = \Re[E(z)] + \beta x + \alpha,$$

showing that the point of affix $D(z)$ lies always to the right of $E(z)$. Proceeding now as in the proof of Theorem 3.3 (details are omitted), it is easy to see that $E(z)/z$ has no zeros in the region $\mathcal{V}$ from which we remove a small semicircle of radius $\gamma + \varepsilon$, centered at the origin and located in the right half-plane, where ε is an arbitrary small positive number. Hence, $D(z)$ cannot vanish in $\mathcal{V}$, since this would contradict the equality of the number of zeros in the region $\mathcal{V}$. The theorem is proved. ∎

5. Partial string stability. Car-following scenarios can be analyzed from the scope of interconnected systems theory as a cascaded sequence. Given this, the bandwidth and time delay of inter-systems coupling determine how an exogenous input propagates along the string in upstream direction. String stability concerns only whether the energy of this input increases or not as during the propagation. More specifically, it only takes into account the propagation function's $\mathcal{H}_\infty$-norm to classify the sequence as string stable or not. This has been sufficient for most automated car-following systems and human car-following models. Nevertheless, the details of the propagation along the frequency spectrum are ignored in the above definition. The study of the modulus of the transfer function of human car-following models with reaction delay led us to introduce a third category, namely partial string stability. This intends to describe more precisely how the oscillations are propagated upstream, in addition to knowing whether they are amplified or attenuated.

String stability is easy to investigate when the reaction time is $\tau = 0$: either it holds, or $|Q(iy)| > 1$ in a neighborhood of 0. When $\tau > 0$, there is a third possibility, that we introduce below.

DEFINITION 5.1 (Partial string stability).
Let $y_c = \min\{y \geq 0 : |Q(iy)| > 1\}$. *The following classification holds*

1. *if* $y_c = \infty$, *the system is* string stable*;*
2. *if* $0 < y_c < \infty$, *the system is* partially string stable*;*
3. *if* $y_c = 0$, *the system is* string unstable.

Note that, since

$$F(y) \stackrel{\text{def}}{=} |Q(iy)|^2 = \frac{\alpha^2 + \beta^2 y^2}{(\alpha - y^2 \cos y)^2 + (\sin y + \delta y)^2}, \tag{5.1}$$

the modulus of the transfer function becomes eventually less than 1 as $y \to \infty$:

$$\limsup_{y \to \infty} F(y) \leq \frac{\beta^2}{\delta^2} = \frac{\beta^2}{(\beta + \gamma)^2} \leq 1.$$

On the one hand, a string unstable system amplifies the energy of a disturbance as it propagates upstream for all frequency modes below a certain frequency bandwidth. On the other hand, a partially string stable system shows a band-pass filter behavior, where only a finite range of medium frequencies are amplified. This distinction can be leveraged both to describe more accurately the traffic shock waves dynamics and to mitigate their effects.

Partial string stability covers cases where $|Q(iy)|$ can be greater than 1 for some $|y| > y_c$. Accordingly, the next step will be to analyze the modulus of $Q(z)$ on the imaginary axis, especially its position with respect to the value 1. As the reader will note, finding exact necessary and sufficient conditions for string stability in the parameter domain is a thorny problem, which we intend to tackle hereafter.

5.1. Conditions for partial string stability. In the next theorem, we give in particular the maximum interval containing all possible frequencies y satisfying $|Q(iy)| = 1$.

THEOREM 5.2. *The following properties hold.*

(i) The system is either string stable or partially string stable if, and only if,

$$2\alpha < \delta^2 - \beta^2 \stackrel{\text{def}}{=} \mu. \tag{5.2}$$

This condition implies also stability if $\delta < a \sin a \approx 1.04098$, *where* $a = \arccos(\sqrt{2} - 1)$.

(ii) The system is string stable if

$$2\alpha < \mu \quad \text{and} \quad \delta < \frac{1}{2}. \tag{5.3}$$

(iii) Assuming condition (5.2), any critical y_c *such that* $|Q(iy_c)| = 1$ *satisfies the inequalities*

$$\sqrt{Y_-} < y_c < \sqrt{Y_+}, \text{ with } Y_\pm = \beta^2 + \delta^2 \pm 2\sqrt{\beta^2 \delta^2 + \alpha^2}. \tag{5.4}$$

One can check that condition (5.2) does not depend on $\tau > 0$ and is the same as condition (10) in [6], where $\tau = 0$, in which case (5.2) is actually necessary and sufficient for string stability.

Proof. From the definition of $F(y)$ given in (5.1), an easy algebra yields

$$\frac{1-F(y)}{y^2} = \frac{G(y)}{|D(iy)|^2}, \quad \text{with } G(y) \stackrel{\text{def}}{=} y^2 - 2(\delta y \sin y + \alpha \cos y) + \mu, \tag{5.5}$$

and now condition (5.2) becomes immediate, since

$$F(0) = 1, \quad F'(0) = \lim_{y\to 0} \frac{F(y)-1}{y} = 0, \quad \lim_{y\to 0} \frac{F(y)-1}{y^2} = \frac{F''(0)}{2} = \frac{2\alpha-\mu}{\alpha^2}.$$

The condition $\mu > 2\alpha$, rewritten as $\delta^2 > \beta^2 + 2\alpha$, implies $\delta^2 > 2\alpha$, in which case the couple (δ, α) lies inside the domain K_0 defined in Theorem 3.3. By using (3.1), one checks easily that, in the parameter space, the parabola $\alpha = \delta^2/2$ crosses the curve $\mathcal{L}_0$ when

$$\begin{aligned} y^2 \sin^2 y = 2y^2 \cos y &\iff \cos^2 y + 2\cos y - 1 = 0 \\ &\iff y = \arccos(\sqrt{2} - 1), \end{aligned}$$

which gives $\delta = y \sin y \approx 1.04098$, showing property (i). On the other hand, since, for all $y > 0$,

$$G(y) = y(y - 2\delta \sin y) + \mu - 2\alpha \cos y > y^2(1 - 2\delta) + \mu - 2\alpha,$$

equation (5.5) has no real root if $\{\delta < 1/2\} \wedge \{\mu > 2\alpha\}$, proving (5.3) and (ii). As for (iii), we note first

$$G(0) = \mu - 2\alpha, \quad G'(0) = 0, \quad G''(0) = 2(1 + \alpha - 2\delta).$$

The problem of the existence of y_c in (5.4) can be formulated in terms of the intricate following puzzle.

> *For given parameters α, β, γ, find the conditions ensuring the existence of y_c, the smallest positive root of $G(y) = 0$*, where $G(y)$ was defined by equation (5.5).

To this end, let us introduce the family of parametrized trinomials $H(y, z)$, where z stands for a positive real parameter, and

$$H(y, z) = y^2 - 2\delta y \sin z - 2\alpha \cos z + \mu. \tag{5.6}$$

Setting $t = \tan(z/2)$ and using the classical formulas

$$\sin z = \frac{2t}{1+t^2}, \quad \cos z = \frac{1-t^2}{1+t^2},$$

one checks easily that the equation $H(y, z) = 0$ corresponds in a one-to-one way to the function $K(y, t) = 0$, where

$$\begin{aligned} K(y,t) &= (y^2 + 2\alpha + \mu)t^2 - 4\delta t y + y^2 - 2\alpha + \mu \\ &= (1+t^2)y^2 - 4\delta t y + (\mu + 2\alpha)t^2 + \mu - 2\alpha. \end{aligned} \tag{5.7}$$

In the sequel $K(y, t)$ will be viewed, *ad libitum*, either as a trinomial in y or a trinomial in t. Hence, $G(y) \equiv H(y, y) = 0$ is plainly equivalent to the system

$$\begin{cases} K(y,t) = 0, \\ t = \tan(y/2). \end{cases} \tag{5.8}$$

Since $G(y)$ is an even function of y, we shall only look for its positive roots, remarking that if (y,t) satisfies (5.8), then $y>0 \Rightarrow t>0$. This means that we can restrict ourselves to the roots of G of the form $y=y_1+2k\pi$ with $0<y_1<\pi$ and $k\geq 0$.

At our convenience, we shall use the variables $Y \overset{\text{def}}{=} y^2$ and $T \overset{\text{def}}{=} t^2$. Also, according to (5.2), it is worth recalling that $\mu=\delta^2-\beta^2$. Then, the reduced discriminant of $K(y,t)=0$, considered as a quadratic equation in t, is equal to

$$A(Y) \overset{\text{def}}{=} -Y^2+2(2\delta^2-\mu)Y+4\alpha^2-\mu^2, \tag{5.9}$$

which has two real positive roots Y_+, Y_-, where

$$Y_-=\beta^2+\delta^2-2\sqrt{\beta^2\delta^2+\alpha^2}, \quad Y_+=\beta^2+\delta^2+2\sqrt{\beta^2\delta^2+\alpha^2}. \tag{5.10}$$

Quite similarly, the reduced discriminant of $K(y,t)=0$, considered now as a quadratic equation in y, is equal to

$$B(T) \overset{\text{def}}{=} -(2\alpha+\mu)T^2+2(2\delta^2-\mu)T+2\alpha-\mu, \tag{5.11}$$

which has two real positive roots T_+, T_-, where

$$T_-=\frac{Y_-}{2\alpha+\mu}, \quad T_+=\frac{Y_+}{2\alpha+\mu}.$$

Hence, any possible positive solution (y,t) of (5.8) necessarily satisfies the inequalities

$$\sqrt{Y_-}\leqslant y\leqslant\sqrt{Y_+}, \quad \sqrt{T_-}\leqslant t\leqslant\sqrt{T_+}, \tag{5.12}$$

since in this case $A(Y)$ and $B(T)$, respectively given by (5.9) and (5.11), are positive, which proves in particular (5.4), concluding the proof of the theorem. □

Remark 5.3. It is worth illustrating on a toy example the existence of a set of positive parameters α,β,γ, for which $F(y)$ becomes strictly larger than 1 for some y. Taking for instance $y=\pi/4$, one can check that the quantity

$$G(\pi/4)=\gamma^2+\left(2\beta-\frac{\pi\sqrt{2}}{4}\right)\gamma+\frac{\pi^2}{4}-\sqrt{2}\left(\frac{\beta\pi}{4}+\alpha\right)$$

can be rendered negative for $\beta=\frac{\pi}{\sqrt{2}}$, $(\gamma,\alpha)\in[0,\gamma_0]\times[0,\alpha_0]$, the constraint $\mu>2\alpha$ being satisfied in these intervals. Incidentally, one might think that the curvature of G at the origin (i.e. the sign of $G''(0)$) plays a decisive role in the way $F(y)$ reaches and exceeds 1. Actually, it is easy to check that this is not the case.

Remark 5.4. By using the elementary inequalities

$$y-y^3/6\leq\sin y\leq y, \quad 1-y^2/2\leq\cos y\leq 1-y^2/2+y^4/24,$$

we get the following easy bounds, valid for all $y>0$,

$$\frac{\delta}{3}y^4\geq G(y)-(1+\alpha-2\delta)y^2+2\alpha-\mu\geq-\frac{\alpha}{12}y^4,$$

offering practical help to find concrete sufficient conditions for the existence of real zeros of the function G.

5.2. About a surface in the parameter domain ensuring partial string stability. From now on, we assume that the system is stable and that condition (5.2) holds. The characterization of the exact parameter regions by a separating surface $\mathcal{S}$ that discriminates between existence and non existence of positive roots for equation (5.5) proves to be very difficult. Hereafter, we propose two theoretical directions. Both of them have a geometrical flavor, and rely on an intermediate parametrization of the equation $G(y) = 0$.

- In Section 5.2.1, $\mathcal{S}$ is characterized in the state space (α, δ, μ) by saying that a system of three equations with two unknowns must admit a solution. This is tantamount to analyze the contact point of a quartic curve with the tangent curve $t = \tan(y/2)$.
- In Section 5.2.2, we propose a similar approach, by using a different parametrization, which leads to analyze the contact point of a parabola with the pseudolinear curve $z = 2(\delta y \sin y + \alpha \cos y)$. We provide a simple parametric description of $\mathcal{S}$ in the state space (α, β, γ). We also push the argument by showing that μ, viewed as a function of α and δ, satisfies a nonlinear partial differential equation of first order, the solution of which describes $\mathcal{S}$ in the parameter space (α, δ, μ).

5.2.1. Intersection of a quartic curve with a tangent curve. Finding the exact necessary and sufficient conditions for string stability is tantamount to locate the closed curve $K(y, t) = 0$ with respect to the periodic curve $t = \tan(y/2)$, in the region defined by (5.12) in the (y, t)-plane, see Fig. 5.1. In particular, one must specify their possible tangency points, obtained by means of the additional relation

$$\frac{\partial K(y,t)}{\partial t} + \frac{d\tan(y/2)}{dy} = 0,$$

which, by using the identity

$$\frac{d\tan(y/2)}{dy} = \frac{1+t^2}{2},$$

yields the algebraic equation

$$t(1+t^2)y^2 + 2(1-\delta)(t^2+1)y + (2\alpha+\mu)t(1+t^2) - 4\delta t = 0. \tag{5.13}$$

The system made by (5.8) and (5.13) contains three equations (two of them being algebraic) with only two unknowns, so that there exists a relationship between the parameters (α, δ, μ), which describes the surface $\mathcal{S}$. The related algebra (for instance all admissible parameter triples must be positive) to find the exact solution, as well as numerical implementations, are rather tedious and this question remains a pending issue.

5.2.2. Intersection of a parabola with a linear-sinusoidal curve. Here the idea is to analyze the first possible tangency point in the (y, z)-plane of the two curves (see Fig. 5.2)

$$\begin{cases} z = y^2 + \mu, & \text{(parabola)} \\ z = 2(\delta y \sin y + \alpha \cos y). \end{cases} \tag{5.14}$$

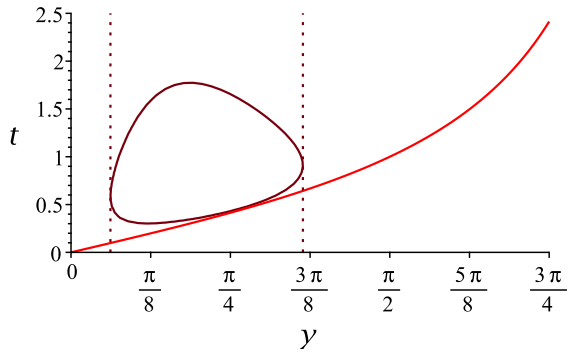

FIG. 5.1. *Representation of $K(x,t) = 0$ and $t = \tan(y/2)$ for arbitrary parameter values $\alpha = 0.074$, $\beta = 0.45$ and $\gamma = 0.235$, chosen so that the curves are tangent. The vertical dotted lines mark the bounds (5.4).*

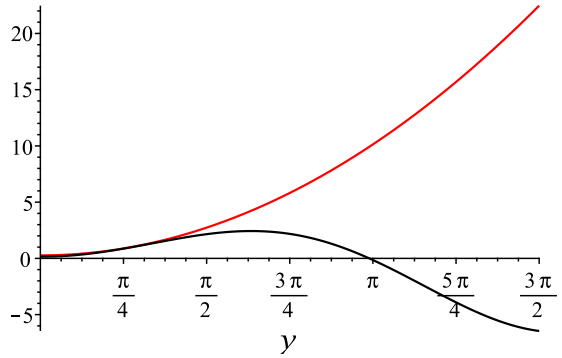

FIG. 5.2. *The two functions defined in (5.14), for the same parameter values as in Fig. 5.1.*

By identifying the normal vectors at the contact point of the two curves, we immediately obtain the following system

$$\begin{cases} \delta y \cos y + (\delta - \alpha) \sin y = y, \\ 2(\alpha \cos y + \delta y \sin y) = y^2 + \mu. \end{cases} \tag{5.15}$$

This system can be used for representation purposes. Indeed, expressing δ and μ in terms of the original α, β and γ parameters, it appears that (5.15) is a linear system of equations in α and β, which gives

$$\begin{cases} \alpha &= \dfrac{1}{2} \dfrac{(\gamma^2 + y^2) \sin y + \big((\gamma^2 - y^2) \cos y - 2\gamma\big) y}{(\gamma - \cos y) \sin y - y}, \\ \beta &= \dfrac{1}{2} \dfrac{(2\gamma \cos y - \gamma^2 - y^2) \sin y + 2y(\gamma - \cos y)}{(\gamma - \cos y) \sin y - y}. \end{cases} \tag{5.16}$$

Fig. 5.3 uses this parametric definition in (y, γ) to represent the separating surface $\mathcal{S}$ in the parameter space (α, β, γ).

Our next goal is to exhibit a partial differential equation representing the surface

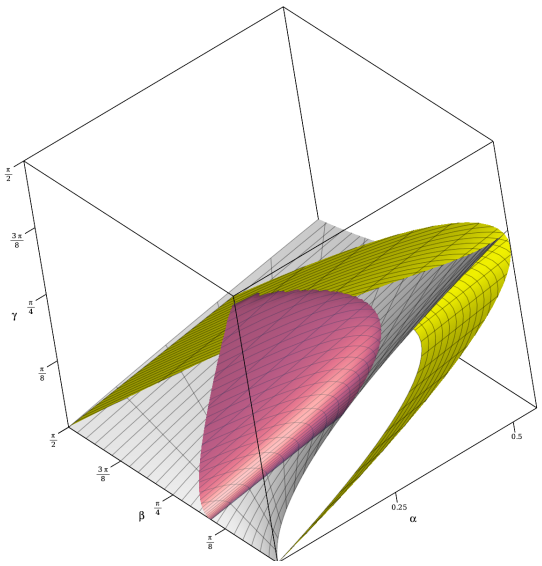

FIG. 5.3. *3D representation in the (α, β, γ) space of the separation between several regimes. The yellow cylinder is equivalent to K_0 and encloses the stability region described in Theorem 3.3; in the domain beyond the grey surface $2\alpha = \mu \equiv \gamma(2\beta + \gamma)$, the system is string unstable; finally, the red surface $\mathcal{S}$ separates string stability (in front) from partial string stability.*

$\mathcal{S}$ in parameter space (α, δ, μ). To this end, we rewrite (5.15) as

$$\begin{cases} \cos y = \dfrac{(\alpha+\delta)y^2 + \mu(\alpha-\delta)}{2[\delta^2 y^2 + \alpha(\alpha-\delta)]}, \\ \sin y = \dfrac{\delta y^3 + (\mu\delta - 2\alpha)y}{2[\delta^2 y^2 + \alpha(\alpha-\delta)]}. \end{cases} \tag{5.17}$$

We shall consider μ and y as functions of the two independent variables α and δ. Then, upon combining the first equation of (5.15) with (5.17), we get

$$\begin{aligned} \frac{\partial y}{\partial \alpha} &= \frac{\sin y}{(2\delta - \alpha)\cos y - \delta y \sin y - 1} \\ &= \frac{-y(\delta y^2 + \mu\delta - 2\alpha)}{\delta^2 y^4 + (\mu\delta^2 + \alpha^2 - 3\alpha\delta)y^2 + ((\mu+2)\alpha - 2\delta\mu)(\alpha - \delta)}. \end{aligned} \tag{5.18}$$

After some algebra (helped by the Maple software), the second equation of (5.15), allied with (5.18), simplifies to a pleasant homographic function of $Y = y^2$

$$\begin{aligned} \frac{\partial \mu}{\partial \alpha} &= 2\big[y(\delta\cos y - 1) + (\delta - \alpha)\sin y\big]\frac{\partial y}{\partial \alpha} + 2\cos y \\ &= \frac{(\alpha+\delta)Y + \mu(\alpha-\delta)}{\delta^2 Y + \alpha(\alpha-\delta)}. \end{aligned} \tag{5.19}$$

Quite similarly, still starting from (5.15) and (5.17), we get

$$\frac{\partial \mu}{\partial \delta} = \frac{Y(\delta Y + \mu) - 2\alpha}{\delta^2 Y + \alpha(\alpha - \delta)}. \tag{5.20}$$

TABLE 6.1
Parameters for the IDM model

Parameter	value
Desired velocity v_0	$33\,\mathrm{m/s}$
Safe time headway T	$1.5\,\mathrm{s}$
Maximum acceleration a	$1.5\,\mathrm{m/s^2}$
Desired deceleration b	$1.5\,\mathrm{m/s^2}$
Acceleration exponent δ	4
Jam distance s_0	$2\,\mathrm{m}$
Vehicle length ℓ	$5\,\mathrm{m}$
Reaction time τ	$1.5\,\mathrm{s}$

Then, eliminating Y between equations (5.19) and (5.20), we obtain that the function $\mu(\alpha,\delta)$ satisfies the following nonlinear partial differential equation

$$\frac{\partial\mu}{\partial\delta}\Big(-\frac{\partial\mu}{\partial\alpha}\delta^2+\alpha+\delta\Big)=\Big(\alpha\frac{\partial\mu}{\partial\alpha}-\mu\Big)\Big(\delta\frac{\partial\mu}{\partial\alpha}-2\Big), \tag{5.21}$$

which, for prescribed initial conditions, has a unique solution. In our case, the solution of (5.21) satisfying (5.15) is the one containing the line $(\alpha=2t,\delta=t,\mu=4t)$, $t\in\mathbb{R}$. Then, to select the convenient portions of this surface, we have to take into account the constraints

$$0\le 2\alpha\le\mu\le\delta^2, \tag{5.22}$$

remembering from equation (2.5) that $\mu=\delta^2-\beta^2=\gamma(2\beta+\gamma)$. We leave the formal solution of (5.21) as an open problem.

Remark 5.5. It is worth to emphasize that the surface $\mathcal{S}$ could also be described by considering α as a function of the two independent parameters β,γ. This leads again to a nonlinear partial differential equation which, unfortunately, is rather indigestible!

6. Application to the Intelligent Driver Model. Although our results are usable with any local linearization of a car-following model of the form (2.1), it will be convenient to use a delayed version of the Intelligent Driver Model (IDM). This model is defined through the following function f, which is clearly of the form (2.1).

$$f(\Delta x,\Delta v,v)=a\left[1-\left(\frac{v}{v_0}\right)^{\delta}-\left(\frac{s^*(v,\Delta v)}{\Delta x-\ell}\right)^2\right],$$
$$\text{with } s^*(v,\Delta v)=s_0+vT-\frac{v\cdot\Delta v}{2\sqrt{a\,b}}.$$

It is easy to compute the equilibrium interdistance Δx^* as a function of v^*,

$$\Delta x^*=\frac{s_0+v^*T}{\sqrt{1-(v^*/v_0)^{\delta}}}+\ell,$$

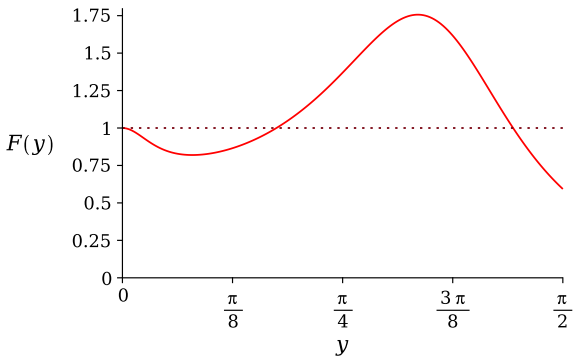

FIG. 6.1. *Representation of the function* $F(y) = |Q(iy)|^2$ *for the Intelligent Driver Model with parameters given in Table 6.1 and* $v^* = 25\,\mathrm{m/s}$.

and the parameters of the linear differential equation (2.3) are thus

$$k_{dx} = \frac{\partial f}{\partial \Delta x}(\Delta x^*, 0, v^*) = \frac{2a(s_0 + v^*T)^2}{\Delta x^{*3}},$$
$$k_{dv} = \frac{\partial f}{\partial \Delta v}(\Delta x^*, 0, v^*) = \frac{av^*(s_0 + v^*T)}{\Delta x^{*2}\sqrt{ab}},$$
$$k_v = -\frac{\partial f}{\partial v}(\Delta x^*, 0, v^*) = a\Big[\frac{\delta}{v^*}\Big(\frac{v^*}{v_0}\Big)^{\delta} + \frac{2T(s_0 + v^*T)}{\Delta x^{*2}}\Big].$$

In this section we use the set of parameters given in Table 6.1, which is realistic according to [30]. As far as the reaction time is concerned, several studies suggest that the choice of $\tau = 1.5$ is quite reasonable, although the actual value depends on the circumstances [11, 17]. In order to see what happens on a particular example, let us pick an equilibrium speed $v^* = 25\,\mathrm{m/s}$. It is easy to solve explicitly the equilibrium equation (2.2), and find $\Delta x^* = 48.23\,\mathrm{m}$. Then the respective parameters of the linear system are $\alpha = 0.0975$, $\beta = 0.6366$ and $\gamma = 0.2332$. In this case, $|Q(iy)| > 1$ if and only if $y \in [0.5379, 1.5116]$ (see Fig. 6.1).

Beyond the string stable and string unstable cases highlighted in [6, 31], the above example shows that introducing a reaction time can lead to a hybrid situation, which is string stable for values of y below some threshold. More generally, it is possible to explore the parameter space of IDM by varying v^* and τ, while studying the slope at frequency zero and the L^∞ norm of the propagation function $F(iy)$. The top graph of Fig. 6.2 shows the string stability classification of the linearized IDM depending on these parameters. One sees that a sufficiently large reaction delay may trigger a shock wave, even for a driver with string stable car-following characteristics. As expected, the limit for string instability does not depend on τ. The same classification is shown in the bottom panel of Fig. 6.2 in the (δ, α) plane. For our chosen parameters of IDM, both full and partial string stability are clearly in the stability domain K_0.

7. Conclusion and future research. The addition of a reaction time to some car-following models renders the analysis more intricate. Not only a nontrivial instability region appears, but in addition the string stability classification can be enriched by an intermediate class, named *partial string stability*. This seems interesting because it permits new control strategies for string of vehicles, in particular when a few automated vehicles are inserted in a flow of human-driven ones. Indeed, it becomes

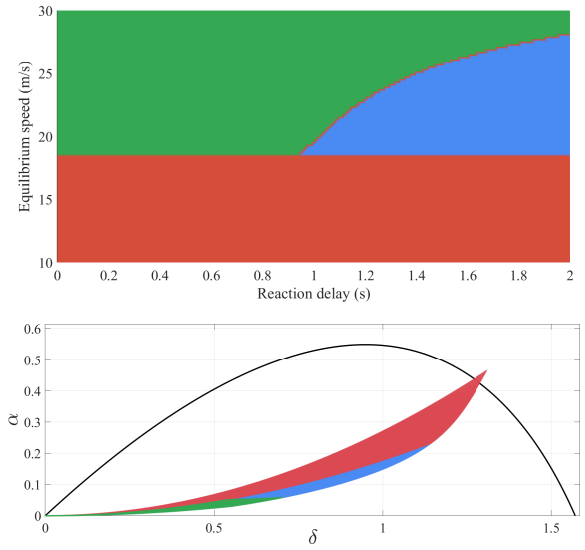

FIG. 6.2. *Top: classification of string stability as a function of equilibrium speed v^* and reaction-time delay τ. Possible states are string stable (green), partially string stable (blue) and string unstable (red). Bottom: the same information set in the (δ, α) plane.*

possible to take advantage of the range $0 < |y| < y_c$, where $|Q(iy)| < 1$, to regulate the amplification of potential shock waves.

This study is intended to be a foundation of a larger work on traffic stabilization by means of a fleet of cooperative automated vehicles. Several authors [6, 7, 9, 31] have suggested that it is possible to use a small proportion of automated vehicles (AV) to regulate a traffic regime which exhibits string instability. We intend to extend this idea in two directions.

1. By taking into account the reaction-time delay, which can lead to stop-and-go traffic jams. The notion of partial string stability could be exploited by the traffic damping car-following controller, since such controllers can be designed to attenuate more significantly the spectral band that shows disturbance amplification in the resulting model — e.g. as that of Section 6.
2. By introducing communication between automated vehicles as in [7], but relying on a car-following model rather than on a first-order fluid model. The addition of connected AVs enables the detection of shock waves downstream of the automated ego-vehicle and can provide an anticipated signal for the car-following controller.

While the focus of the present work is on the behavior of human-driven vehicles at microscopic level, the next steps will be to tackle shock wave analysis along the lines of [1, 27] and to devise adapted traffic-stabilizing control strategies. In this respect, an interesting problem would to find a macroscopic model (very likely of second order), able to incorporate the stability analysis of the transfer function $Q(z)$. We plan to address this issue in a near future.

Acknowledgments. The authors thank Alin Bostan (Inria-Saclay Research Center) for bringing reference [3] to their attention, and the anonymous referees for their remarks and suggestions.

REFERENCES

[1] A. Aw, A. Klar, M. Rascle, and T. Materne, *Derivation of continuum traffic flow models from microscopic follow-the-leader models*, SIAM J. Appl. Math., 63 (2002), pp. 259–278.

[2] M. Bando, K. Hasebe, A. Nakayama, A. Shibata, and Y. Sugiyama, *Dynamical model of traffic congestion and numerical simulation*, Phys. Rev. E, 51 (1995), pp. 1035–1042.

[3] R. Bellman and K. L. Cooke, *Differential-Difference Equations*, Academic Press, New York, 1963.

[4] R. E. Chandler, R. Herman, and E. W. Montroll, *Traffic dynamics: studies in car following*, Oper. Res., 6 (1958), pp. 165–184.

[5] R. M. Corless, G. H. Gonnet, D. E. G. Hare, D. J. Jeffrey, and D. E. Knuth, *On the Lambert W function*, Adv. Computat. Math., 5 (1996), pp. 329–359.

[6] S. Cui, B. Seibold, R. Stern, and D. B. Work, *Stabilizing traffic flow via a single autonomous vehicle: possibilities and limitations*, in IEEE Intell. Veh. Symp., June 2017, pp. 1336–1341.

[7] M. Forster, R. Frank, M. Gerla, and T. Engel, *A cooperative advanced driver assistance system to mitigate vehicular traffic shock waves*, in IEEE Conf. Comput. Commun., April 2014, pp. 1968–1976.

[8] D. Gazis, R. Herman, and R. W. Rothery, *Nonlinear follow-the-leader models of traffic flow*, Oper. Res., 9 (1961), pp. 545–567.

[9] V. Giammarino, S. Baldi, P. Frasca, and M. L. Delle Monache, *Traffic flow on a ring with a single autonomous vehicle: An interconnected stability perspective*, IEEE Trans. Intell. Transp. Syst., 22 (2021), pp. 4998–5008.

[10] P. G. Gipps, *A behavioural car-following model for computer simulation*, Transp. Res. Part B Methodol., 15 (1981), pp. 105–111.

[11] M. Green, *"How long does it take to stop?" Methodological analysis of driver perception-brake times*, Transp. Hum. Factors, 2 (2000), pp. 195–216.

[12] D. Helbing, *Traffic and related self-driven many-particle systems*, Rev. Mod. Phys., 73 (2001), pp. 1067–1141.

[13] B. S. Kerner, *Breakdown in Traffic Networks. Fundamentals of Transportation Science*, Springer, 2017.

[14] A. Kesting and M. Treiber, *How reaction time, update time, and adaptation time influence the stability of traffic flow*, Comput.-Aided Civ. Infrastruct. Eng., 23 (2008), pp. 125–137.

[15] V. V. Kurtc and I. E. Anufriev, *Car-following model with explicit reaction-time delay: linear stability analysis of a uniform solution on a ring*, Math. Models Comput. Simul., 9 (2017), pp. 679–687.

[16] M. Lavrentiev and B. Chabat, *Méthodes de la théorie des fonctions d'une variable complexe*, Mir, Moscou, 2nd ed., 1977.

[17] D. V. McGehee, E. N. Mazzae, and G. H. S. Baldwin, *Driver reaction time in crash avoidance research: Validation of a driving simulator study on a test track*, Proc. Hum. Factors Ergon. Soc. Annu. Meet., 44 (2000), pp. 3–320–3–323.

[18] L. A. Pipes, *An operational analysis of traffic dynamics*, J. Appl. Phys., 24 (1953), pp. 274–281.

[19] J. Ploeg, N. van de Wouw, and H. Nijmeijer, *$\mathcal{L}_p$ string stability of cascaded systems: Application to vehicle platooning*, IEEE Trans. Control Syst. Technol., 22 (2014), pp. 786–793.

[20] L. Pontryagin, *On the zeros of some elmentary transendental functions*, Amer. Math. Soc. Transl., 1 (1955), pp. 95–110.

[21] W. J. Schakel, B. Van Arem, and B. D. Netten, *Effects of cooperative adaptive cruise control on traffic flow stability*, in IEEE Intell. Transp. Syst., 2010, pp. 759–764.

[22] R. E. Stern et al., *Dissipation of stop-and-go waves via control of autonomous vehicles: Field experiments*, Transp. Res. Part C Emerging Technol., 89 (2018), pp. 205–221.

[23] Y. Sugiyama et al., *Traffic jams without bottlenecks—experimental evidence for the physical mechanism of the formation of a jam*, New J. Phys., 10 (2008).

[24] D. Swaroop and J. K. Hedrick, *String stability of interconnected systems*, IEEE Trans. Autom. Control, 41 (1996), pp. 349–357.

[25] E. Titchmarsh, *The Theory of Functions*, Oxford University Press, New York, 2nd. ed., 1997.

[26] T. Toledo, *Driving behaviour: models and challenges*, Transp. Rev., 27 (2007), pp. 65–84.

[27] A. Tordeux, G. Costeseque, M. Herty, and A. Seyfried, *From traffic and pedestrian follow-the-leader models with reaction time to first order convection-diffusion flow models*, SIAM J. Appl. Math., 78 (2018), pp. 63–79.

[28] M. Treiber and D. Helbing, *Memory effects in microscopic traffic models and wide scattering in flow-density data*, Phys. Rev. E, 68 (2003), p. 046119.

[29] M. Treiber, A. Hennecke, and D. Helbing, *Congested traffic states in empirical observations*

and microscopic simulations, Phys. Rev. E, 62 (2000), p. 1805.
[30] M. Treiber and A. Kesting, *Traffic Flow Dynamics: Data, Models and Simulation*, Springer, Berlin, Heidelberg, 2013.
[31] C. Wu, A. Bayen, and A. Mehta, *Stabilizing traffic with autonomous vehicles*, in IEEE Int. Conf. on Robotics and Automation, 05 2018, pp. 1–7.